

Electrochemical reduction of Tm ions in LiCl-KCl melt at liquid Zn electrodes*

YAN Yong-De (颜永得),^{1,2,†} LI Xing (李星),² XUE Yun (薛云),^{1,2,‡} TANG Hao (唐浩),¹
JI De-Bin (纪德彬),² HAN Wei (韩伟),² ZHANG Mi-Lin (张密林),² and ZHANG Zhi-Jian (张志俭)¹

¹*Fundamental Science on Nuclear Safety and Simulation Technology Laboratory,
Harbin Engineering University, Harbin 150001, China*

²*Key Laboratory of Superlight Materials and Surface Technology,
Ministry of Education, College of Materials Science and Chemical Engineering,
Harbin Engineering University, Harbin 150001, China*

(Received May 7, 2014; accepted in revised form July 25, 2014; published online December 20, 2014)

The reduction of Tm(III) on a liquid Zn electrode was investigated in a LiCl-KCl melt via cyclic voltammetry, square wave voltammetry, and open circuit chronopotentiometry. On a liquid Zn electrode, the reduction mechanism of Tm(III) ions is through one step with the exchange of three electrons via the formation of a Zn-Tm alloy. This differs from that on an inert electrode, as the reduction is Tm(III) ions were though two consecutive steps. Galvanostatic electrolysis was carried out at a liquid Zn electrode at different current densities in a LiCl-KCl-TmCl₃ melt. The Tm₂Zn₁₇ intermetallic compound was identified in the deposit, except in the Zn phase, by X-ray Diffraction (XRD).

Keywords: Nuclear waste, Electrochemical extraction, Thulium, Molten salt

DOI: [10.13538/j.1001-8042/nst.26.S10309](https://doi.org/10.13538/j.1001-8042/nst.26.S10309)

I. INTRODUCTION

Nuclear energy has been extensively used for electricity production in many nations. However, every year, the spent fuel reprocessing system of a nuclear power station will produce a large quantity of high-level radioactive waste (HLW), which pose a great potential hazard to the environment and offspring. Therefore, the disposal of HLW has attracted much attention. Partitioning and transmutation (P&T) represent nowadays a promising method to dispose of HLW, which can recycle or change of the hazardous radionuclides into less hazardous or shorter lived elements [1–6]. However, before this transmutation, it is required to separate the minor actinides (MAs) from other fission products (FPs), especially the rare earth fission products (RE). Molten salt related to electrochemical techniques, which are known as pyrochemical techniques, have been widely studied to investigate the recovery of Ans separated from RE for decades.

In this paper, the electrochemical behavior of Tm is investigated at a liquid Zn electrode, not only because it is present in a small amount in the nuclear waste, but also for the similar electrochemical behavior as Am in molten salt [7]. However, the basic experimental data of Am in molten alkali chlorides are scarce, mainly due to the limited availability of AmCl₃ and its intense radioactivity. The similarities of

Tm and Am in molten salt are as follows [7–13]: (1) They both have two stable forms in molten salt, Tm(III)/Tm(II) and Am(III)/Am(II), respectively. (2) The reduction potentials of Tm(II) and Am(II) are more positive than that of a common solvent, such as Li and Na. As for RE elements Sm, Eu, and Yb, their deposition potentials are similar or more negative than that of Li and Na. (3) The reduction mechanism of Tm(III) and Am(III) are related to the cathode electrode materials. On an inert electrode (W), Tm(III) and Am(III) ions are reduced to metallic Tm and Am through two consecutive steps: (i) Tm(III) + e[−] ↔ Tm(II); (ii) Tm(II) + 2e[−] ↔ Tm(0), and (i) Am(III) + e[−] ↔ Am(II); (ii) Am(II) + 2e[−] ↔ Am(0). Whereas, for Am, in a CaCl₂-NaCl melt, when liquid Al is used as a working electrode, Am(III) ions were reduced into Am(0) though one step, with the exchange of three electrons [13]. For Tm, in a LiCl-KCl and NaCl-2CsCl melt, when solid Al is used as a working electrode, Tm(III) ions were reduced into Tm(0) though one step via the formation of an Al-Tm alloy, with the exchange of three electrons [7, 8]. Therefore, obtaining basic electrochemical data on Tm in molten salt can help in understanding the extraction process of Am.

Compared with molten fluorides, the operating temperature of molten chlorides is much lower. Thus, we suppose Zn is a good cathode due to the lower melting point of pure Zn (about 693 K under atmospheric pressure). Moreover, it is much easier to obtain high purity spongy REE by using reduced-pressure distillation from Zn-Tm alloys.

II. EXPERIMENTAL

A. Preparation and purification of the melt

The mixture of LiCl-KCl (Sinopharm Chemical Reagent Co., Ltd, analytical grade ≥ 99.8% and 99.5%, respective-

* Supported by the High Technology Research and Development Program of China (No. 2011AA03A409), the National Natural Science Foundation of China (Nos. 21103033, 21101040, and 91226201), the Fundamental Research funds for the Central Universities (No. HEUCF141502), the Foundation for University Key Teacher of Heilongjiang Province of China and Harbin Engineering University (Nos. 1253G016 and HEUCFQ1415), and the Special Foundation of China and Heilongjiang Postdoctoral Science Foundation (Nos. 2013T60344 and LBH-TZ0411)

† Corresponding author, y5d2006@hrbeu.edu.cn

‡ Corresponding author, xueyun1045@sina.com

ly) was dried under a vacuum for more than 72 h at 473 K to remove excess water before being used. Tm(III) ions were introduced into a LiCl-KCl melt in the form of anhydrous TmCl_3 (Sinopharm Chemical Reagent Co., Ltd, analytical grade $\geq 99.9\%$), respectively. Before each experiment, HCl was bubbled into the melt to remove oxide ions. And then, Ar gas was bubbled into the melt to remove remanent HCl, oxygen, and water.

B. Electrochemical apparatus and electrodes

Cyclic voltammetry, square wave voltammetry, open circuit chronopotentiometry, and galvanostatic electrolysis were performed using an Autolab PGSTAT 302N potentiostat/galvanostat controlled with the Nova 1.8 software package. The working electrodes are tungsten ($d = 1 \text{ mm}$) and liquid Zn placed in an alumina crucible. The size of the cathode crucible for loading Zn (Aladdin Chemical Co., Ltd., analytical grade 99.99%, about 6–8 g) was 2.2 cm in height and 1.5 cm in diameter. A W wire ($d = 1 \text{ mm}$) placed in an alumina sleeve was immersed in the cathode Zn and used as an electric lead [14]. The surface of W electrodes was polished thoroughly with SiC paper prior to use to remove the oxide film and the impurity of the electrode surface. Moreover, the working electrodes were cleaned by applying an anodic polarization between each measurement. Graphite rod ($d = 6 \text{ mm}$) served as counter electrode. The reference electrode was the Ag^+/Ag couple consisting of AgCl (1.0 wt.%) in LiCl-KCl molten salt dipped into an alundum tube [14].

C. Characterization of Zn-Tm alloys

Zn-Tm alloys were prepared via galvanostatic electrolysis on liquid Zn electrodes. After electrolysis, the samples were washed with ethylene glycol to remove solidified salts attached to the surface of the alloy samples. The samples were then analyzed by X-ray diffraction (XRD) (Rigaku D/max-TTR-III diffractometer) using $\text{Cu}-\text{K}\alpha$ radiation at 40 kV and 150 mA. Scanning electron microscopy (SEM) (JSM-6480A; JEOL Co., Ltd.) was used to analyze the microstructure and micro-zone chemical composition of bulk Zn-Tm alloys.

III. RESULTS AND DISCUSSION

A. Cyclic voltammetry

Figure 1 shows cyclic voltammograms obtained in a LiCl-KCl melt containing different concentrations of TmCl_3 at a Zn electrode at 723 K. In curve 1, two pairs of signals are present. The signals A/A' at about $-0.63/-0.94 \text{ V}$ (vs. Ag/AgCl) are related to the reduction of Zn(II) ions dissolved from a liquid Zn electrode and the oxidation of Zn, respectively. The cathodic signal, C, at roughly -2.00 V is ascribed to the deposition of Li(I) on a liquid Zn electrode forming a Zn-Li alloy. In the reverse scan, the corresponding anodic

signal, C' , is attributed to the dissolution of the Zn-Li alloy. The electrochemical widow of a LiCl-KCl melt on a liquid Zn electrode is limited by the deposition of Zn(II) ions and the formation of a Zn-Li alloy in the cathodic sense. Moreover, the current background of a Zn electrode is larger than that of a solid metal electrode, which is characteristic of liquid metal electrodes [15–17]. After the addition of TmCl_3 in curve 2, a new pair of signals, B/B' , at about $-1.55/-1.23 \text{ V}$ are detected, which should corresponds to the formation/dissolution of a Zn-Tm alloy. The Zn-Tm alloy is formed via the underpotential deposition of Tm(III) on a liquid Zn electrode. With the increase of TmCl_3 in the melt, the deposition potential of Tm(III) ions on a liquid Zn electrode shifts toward positive due to the change of the activity of Tm(III) ions in the melt.

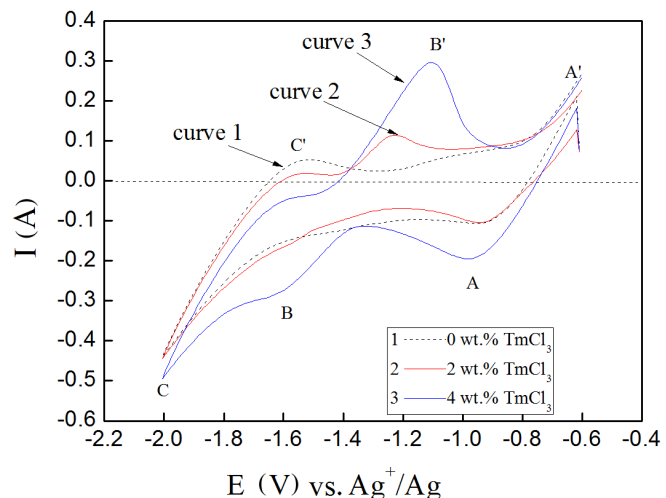


Fig. 1. (Color online) Cyclic voltammograms obtained at liquid Zn electrode ($S = 1.08 \text{ cm}^2$) at 723 K in LiCl-KCl melt (curve 1); LiCl-KCl-TmCl₃ (2 wt.%) melt (curve 2); LiCl-KCl-TmCl₃ (4 wt.%) melt (curve 3); scan rate, 0.2 V/s.

B. Square wave voltammetry

Square wave voltammetry, which is a more sensitive method than cyclic voltammetry, was also conducted to investigate the Tm(III) ions reduction. Fig. 2 shows square wave voltammograms obtained in LiCl-KCl-TmCl₃ (2 wt.%) at a W electrode (dotted line) and a liquid Zn electrode (solid line). As can be seen, on a W electrode (dotted line), two signals, D and E at about -1.59 V and -2.15 V are observed. The signal D with the characteristic of a soluble-soluble electrochemical exchange should correspond to the reduction of Tm(III) to Tm(II) [18–20]. The signal E should be related to the deposition of Tm(II) ions on the W electrode. Whereas on a liquid Zn electrode, only a signal at about -1.43 V is detected, whose potential is a little more positive than that of Tm(III)/Tm(II) on a W electrode (see signal D). As is known, for a soluble-soluble electrochemical exchange, its reduction is not supposed to be related to electrode materials. Therefore, the signal B should not be related to the re-

duction of Tm(III)/Tm(II); but correspond to the reduction of Tm(III)/Tm(0) on a liquid Zn electrode via the formation of a Zn-Tm alloy.

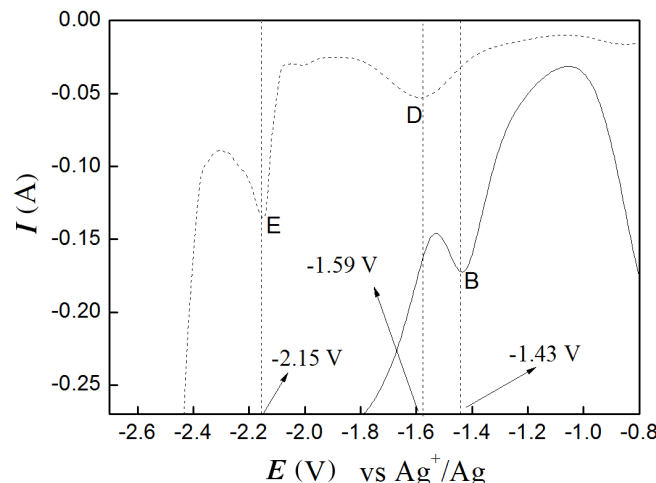


Fig. 2. Square wave voltammograms obtained in $\text{LiCl}-\text{KCl}-\text{TmCl}_3$ (2 wt.%) at a W electrode (dotted line) and liquid Zn electrode (solid line), respectively; pulse height, 25 mV; potential step, 1 mV; frequency, 15 Hz.

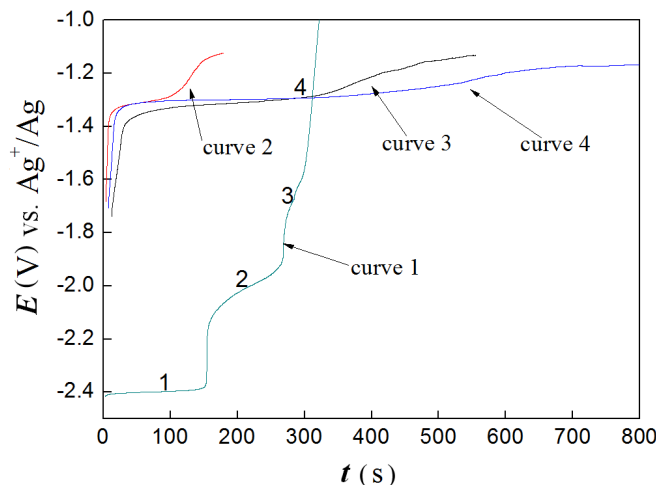


Fig. 3. (Color online) Open circuit chronopotentiometry curves obtained in $\text{LiCl}-\text{KCl}-\text{TmCl}_3$ (2 wt.%) melt at 723 K on a W electrode after potentiostatic electrolysis at -2.5 V for 30 s (curve 1); at liquid Zn electrode after potentiostatic electrolysis at -2.5 V for 2 s (curve 2), 5 s (curve 3) and 10 s (curve 4), respectively.

C. Open circuit chronopotentiometry

Open-circuit chronopotentiometry was employed to further investigate the electrochemical formation of Zn-Tm intermetallic compounds. Fig. 3 shows open circuit chronopotentiometry curves obtained on a W (curve 1) and liquid Zn (curve 2, 3 and 4) electrodes in $\text{LiCl}-\text{KCl}-\text{TmCl}_3$ (2 wt.%)

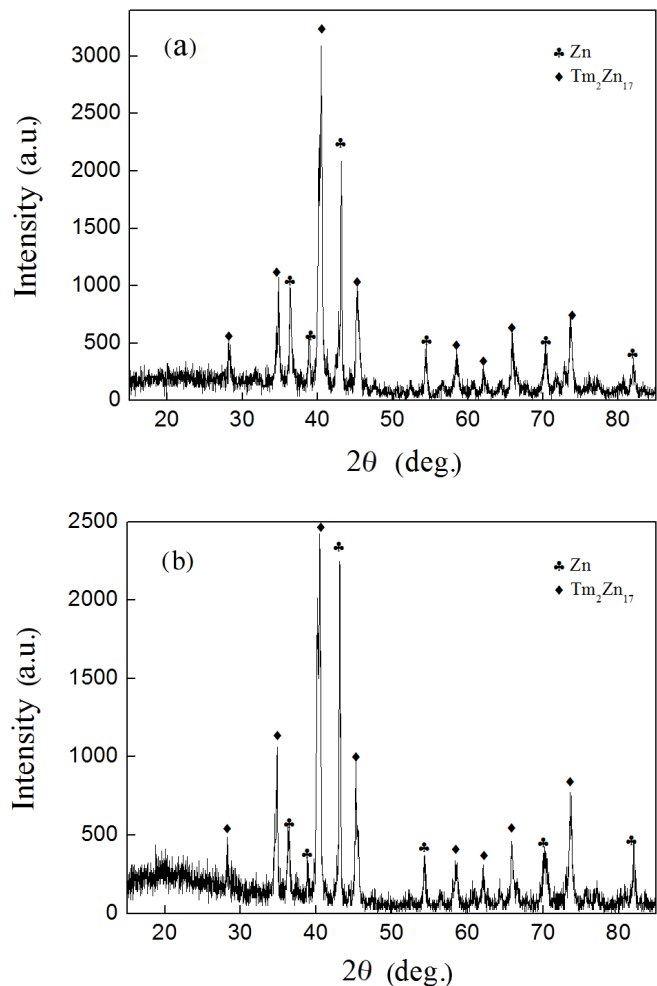


Fig. 4. XRD patterns of deposits obtained in $\text{LiCl}-\text{KCl}-\text{TmCl}_3$ (6 wt.%) melt at 723 K at liquid Zn electrode via galvanostatic electrolysis for 3 h at (a) $200 \text{ mA}/\text{cm}^2$, (b) $300 \text{ mA}/\text{cm}^2$, respectively.

melt. On a W electrode, three plateaus (plateaus 1, 2 and 3) are observed at about -2.40 V , -2.05 V , and -1.60 V corresponding to the deposition of Li(I), deposition of Tm(II)/Tm(0), and reduction of Tm(III)/Tm(II), respectively. When liquid Zn is used as a working electrode, only a plateau (plateau 4) at about -1.30 V is observed, which is attributed to the formation of a Zn-Tm alloy. The deposition potential of Tm(III) at a liquid Zn electrode is about 0.75 V more positive than that on a inert W electrode.

D. Preparation and characterization of Zn-Tm alloys

Based on the above electrochemical analysis, we can conclude that the reduction of Tm(III) ions on a liquid Zn electrode is one step through the exchange of three electrons via the formation of Zn-Tm alloys. Extraction of Tm was carried out at a liquid Zn electrode at 723 K via galvanostatic electrolysis at different current densities. Fig. 4 shows the XRD patterns of deposits obtained in a $\text{LiCl}-\text{KCl}-\text{TmCl}_3$ (6

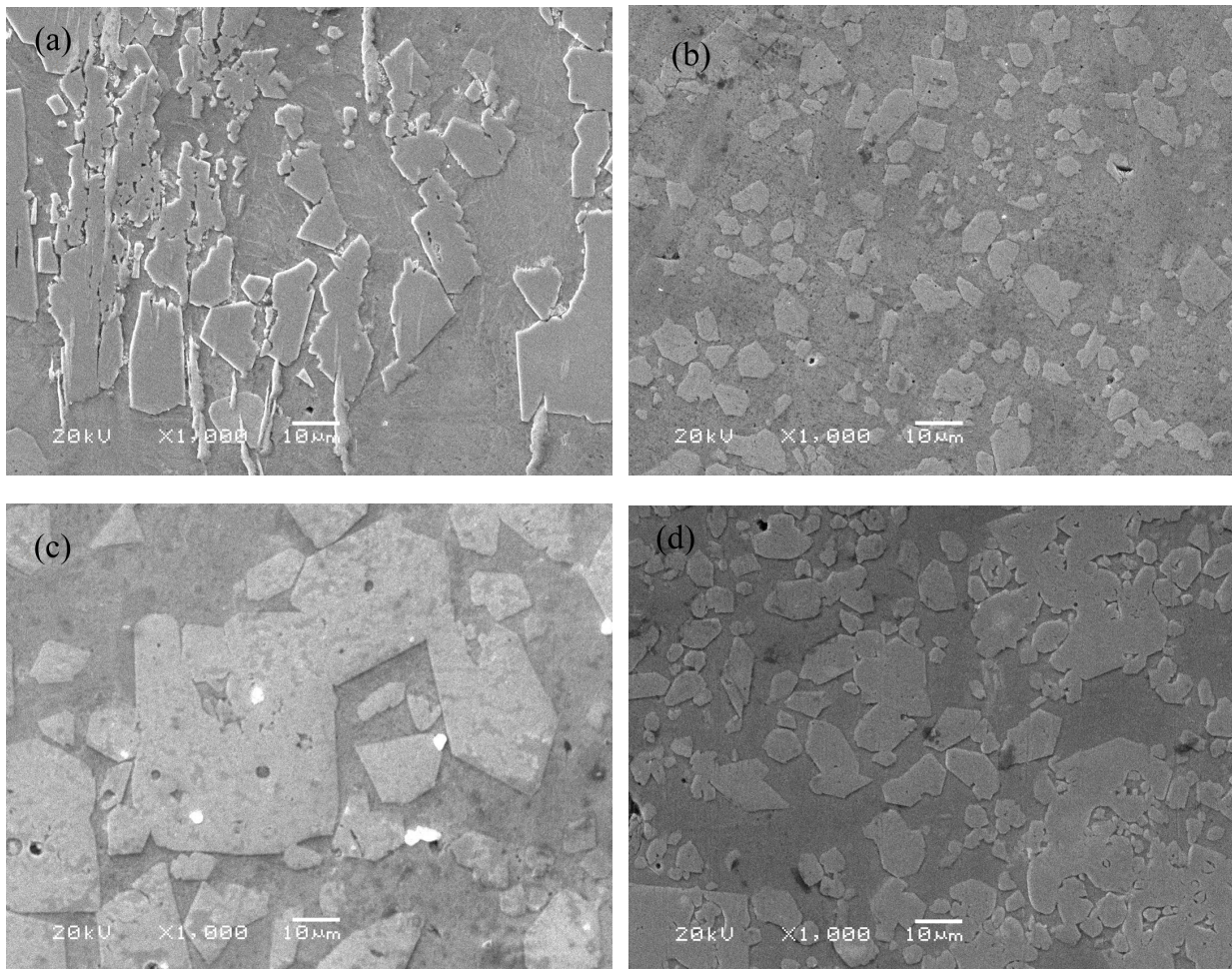


Fig. 5. Cross-sectional SEM (back scattering image) of Zn-Tm alloy obtained in LiCl-KCl-TmCl₃ (6 wt.%) melt at 723 K at liquid Zn electrode via galvanostatic electrolysis at (a) 200 mA/cm², (b) 300 mA/cm² for 3 h, (c) 400 mA/cm² and (d) 500 mA/cm² for 2 h, respectively.

wt.%) melt at 723 K at liquid Zn electrode via galvanostatic electrolysis for 3 h at (a) 200 mA/cm² and (b) 300 mA/cm², respectively. Zn and Tm₂Zn₁₇ phases were detected in the deposits. The Zn phase originates from the liquid Zn electrode. The Tm₂Zn₁₇ phase is formed via the underpotential deposition of Tm(III) in liquid Zn.

Figure 5 shows the cross-sectional SEM (back scattering image) of Zn-Tm alloy obtained in a LiCl-KCl-TmCl₃ (6 wt.%) melt at 723 K at a liquid Zn electrode via galvanostatic electrolysis at (a) 200 mA/cm², (b) 300 mA/cm², (c) 400 mA/cm², and (d) 500 mA/cm², respectively. As can be seen, the alloys are composed of two phases, which are bright and gray zones, respectively. According to our previous study [14], the bright zones correspond to Zn-Tm intermetallic compounds. The convex bulges thought to be the Zn-Tm alloy that precipitate from the Zn matrix during the cooling period due to the low solubility of Tm in a Zn matrix [14]. The shape of convex bulges in samples a, b, c, and d are irregular. The size of the convex bulges are different in the same or different samples, which means that the distribution

of Tm in the deposit and the content of Tm in each sample are different.

IV. CONCLUSION

On an inert W electrode, the reduction of Tm(III) ions were through two consecutive steps: (i) Tm(III) + e⁻ ⇌ Tm(II); (ii) Tm(II) + 2e⁻ ⇌ Tm(0). However, on a liquid Zn electrode, the reduction mechanism of Tm(III) ions is through one step with the exchange of three electrons via the formation of a Zn-Tm alloy. The Zn-Tm alloy formation was confirmed via cyclic voltammetry, square wave voltammetry and open circuit chronopotentiometry on liquid Zn electrodes. The Zn-Tm alloy was prepared via galvanostatic electrolysis at different current densities in a LiCl-KCl melt on liquid Zn electrodes. Tm₂Zn₁₇ and Zn phases were identified in the deposit by XRD. The cross-sectional SEM images (back scattering image) of the Zn-Tm alloys show that the solubility of Tm in Zn is low.

chinaXiv:202306.00314v1

[1] Nishihara K, Nakayama S, Morita Y, *et al.* Impact of Partitioning and Transmutation on LWR High-Level Waste Disposal. *J Nucl Sci Technol*, 2008, **1**: 84–97. DOI: [10.1080/18811248.2008.9711418](https://doi.org/10.1080/18811248.2008.9711418)

[2] González-Romero E.M. Impact of partitioning and transmutation on the high level waste management. *Nucl Eng Des*, 2011, **241**: 3436–444. DOI: [10.1016/j.nucengdes.2011.03.030](https://doi.org/10.1016/j.nucengdes.2011.03.030)

[3] Koch L, Glatz J P, Konings R J M, *et al.* Partitioning and Transmutation Studies at ITU, ITU Annual Report 1999-(EUR 19054)-Partitioning and Transmutation Studies at ITU.

[4] Usuda S, Wei Y Z, Liu R Q. Challenges to develop single-column MA(III) separation from HLLW using R-BTP type adsorbents. *Sci China Chem*, 2012, **55**: 1732–1738. DOI: [10.1007/s11426-012-4691-x](https://doi.org/10.1007/s11426-012-4691-x)

[5] Wei Y Z, Wang X P, Liu R Q. An advanced partitioning process for key elements separation from high level liquid waste. *Sci China Chem*, 2012, **55**: 1726–1731. DOI: [10.1007/s11426-012-4697-4](https://doi.org/10.1007/s11426-012-4697-4)

[6] Han C Y, Ozawa M, Saito M. Resourceability on nuclear fuel cycle by transmutation approach. *Sci China Chem*, 2012, **55**: 1746–1751. DOI: [10.1007/s11426-012-4697-4](https://doi.org/10.1007/s11426-012-4697-4)

[7] Castrillejo Y, Fernández P, Bermejo M R, *et al.* Electrochemistry of thulium on inert electrodes and electrochemical formation of a Tm–Al alloy from molten chlorides. *Electrochim Acta*, 2009, **54**: 6212–6222. DOI: [10.1016/j.electacta.2009.05.095](https://doi.org/10.1016/j.electacta.2009.05.095)

[8] Smolenski V and Novoselova A. Electrochemistry of redox potential of the couple Tm^{3+}/Tm^{2+} and the formation of a Tm–Al alloy in fused $NaCl-2CsCl$ eutectic. *Electrochim Acta*, 2012, **63**: 179–184. DOI: [10.1016/j.electacta.2011.12.089](https://doi.org/10.1016/j.electacta.2011.12.089)

[9] Novoselova A and Smolenski V. The influence of solvent nature on thermodynamic properties of the reaction $Tm(III)+e^- \leftrightarrow Tm(II)$ in molten chlorides. *J Chem Thermodyn*, 2012, **48**: 140–144. DOI: [10.1016/j.jct.2011.12.007](https://doi.org/10.1016/j.jct.2011.12.007)

[10] Novoselova A and Smolenski V. Thermodynamic properties of thulium and ytterbium in fused $NaCl-KCl-CsCl$ eutectic. *J Chem Thermodyn*, 2011, **43**: 1063–1067. DOI: [10.1016/j.jct.2011.02.015](https://doi.org/10.1016/j.jct.2011.02.015)

[11] Novoselova A and Smolenski V. Thermodynamic properties of thulium and ytterbium in molten caesium chloride. *J Chem Thermodyn*, 2010, **42**: 973–977. DOI: [10.1016/j.jct.2010.03.013](https://doi.org/10.1016/j.jct.2010.03.013)

[12] Serp J, Chamelot P, Fourcaudot S, *et al.* Electrochemical behaviour of americium ions in $LiCl-KCl$ eutectic melt. *Electrochim Acta*, 2006, **51**: 4024–4032. DOI: [10.1016/j.electacta.2005.11.016](https://doi.org/10.1016/j.electacta.2005.11.016)

[13] Córdoba G D, Laplace A, Conocar O, *et al.* Determination of the activity coefficient of Am in liquid Al by electrochemical methods. *J Nucl Mater*, 2009, **393**: 459–464. DOI: [10.1016/j.jnucmat.2009.07.002](https://doi.org/10.1016/j.jnucmat.2009.07.002)

[14] Li X, Yan Y D, Zhang M L, *et al.* *J Electrochem Soc*, 2014, **161**: D248–D255. DOI: [10.1149/2.061405jes](https://doi.org/10.1149/2.061405jes)

[15] Castrillejo Y, Bermejo M R, Arocás P D, *et al.* Electrochemical behaviour of praseodymium (III) in molten chlorides. *J Electroanal Chem*, 2005, **575**: 61–74. DOI: [10.1016/j.jelechem.2004.08.020](https://doi.org/10.1016/j.jelechem.2004.08.020)

[16] Kim S H, Paek S, Kim T J. Electrode reactions of Ce^{3+}/Ce couple in $LiCl-KCl$ solutions containing $CeCl_3$ at solid W and liquid Cd electrodes. *Electrochim Acta*, 2012, **85**: 332–335. DOI: [10.1016/j.electacta.2012.08.084](https://doi.org/10.1016/j.electacta.2012.08.084)

[17] Córdoba G D, Laplace A, Conocar O. Determination of the activity coefficient of neodymium in liquid aluminium by potentiometric methods. *Electrochim Acta*, 2008, **54**: 280–288. DOI: [10.1016/j.electacta.2008.08.002](https://doi.org/10.1016/j.electacta.2008.08.002)

[18] Massot L, Chamelot P, Cassayre L, *et al.* Electrochemical study of the $Eu(III)/Eu(II)$ system in molten fluoride media. *Electrochim Acta*, 2009, **54**: 6361–6366. DOI: [10.1016/j.electacta.2009.06.016](https://doi.org/10.1016/j.electacta.2009.06.016)

[19] Gibilaro M, Massot L, Chamelot P. Electrochemical extraction of europium from molten fluoride media. *Electrochim Acta*, 2009, **55**: 281–287. DOI: [10.1016/j.electacta.2009.08.052](https://doi.org/10.1016/j.electacta.2009.08.052)

[20] Castrillejo Y, Fernández P, Medina J, *et al.* Electrochemical extraction of samarium from molten chlorides in pyrochemical processes. *Electrochim Acta*, 2011, **56**: 8638–8644. DOI: [10.1016/j.electacta.2011.07.059](https://doi.org/10.1016/j.electacta.2011.07.059)